Influence of Hydrogen Bonding on the Conformational Changes, the Brill Transition, and Lamellae Thickening in (Co)polyamides

Esther Vinken,[†,||] Ann E. Terry,[†,‡,||] Sven Hoffmann, Bert Vanhaecht,[§] Cor E. Koning,[⊥,§,||] and Sanjay Rastogi*,[†]

Laboratory of Polymer Technology, Department of Chemical Engineering, Eindhoven University of Technology, P.O. Box 513, 5600MB Eindhoven, The Netherlands; ISIS Facility, Rutherford Appleton Laboratory, Chilton, Didcot, Oxfordshire OX11 0QX, United Kingdom; Physical and Colloid Chemistry, Free University of Brussels, Pleinlaan 2, 1050 Brussels, Belgium; Laboratory of Polymer Chemistry, Department of Chemical Engineering, Eindhoven University of Technology, P.O. Box 513, 5600MB Eindhoven, The Netherlands; and Dutch Polymer Institute (DPI), P.O. Box 902, 5600AX Eindhoven, The Netherlands

Received December 16, 2005; Revised Manuscript Received February 3, 2006

ABSTRACT: Copolyamides, based on 1,12-dodecanedicarboxylic acid and different ratios of 1,2-ethylenediamine and piperazine, i.e., PA2,14-*co*-pip,14 as well as the homopolymers PA2,14 and PApip,14 are studied. Incorporation of the piperazine component in the homopolymer PA2,14 reduces the number of hydrogen bonds. This provides a unique opportunity to investigate the influence of hydrogen bonding on the origin of the Brill transition and chain mobility within polymer crystals. Time-resolved conformational, structural, and morphological changes during heating are followed by FTIR spectroscopy, WAXD, and SAXS. The findings are that from 0 to 62 mol % of piperazine the Brill transition occurs in the same temperature region. The transformation is triggered by the conformational changes in the methylene sequences of the main chain, followed by twisting in the methylene sequences next to the amide group. This results in enhanced chain mobility along the *c*-axis, causing lamellar thickening. For 80 mol % of piperazine and higher, no Brill transition is observed. However, conformational changes in the methylene sequences of the main chain occurs, triggering lamellar thickening.

Introduction

Linear aliphatic polyamides, commonly known as nylons, are an important class of the engineering plastics with a wide application range due to their excellent physical and thermal properties. Polyamides have a relatively high melting point in comparison to other polymers because of the hydrogen bonds that form between the recurring amide groups. By varying the density of these hydrogen bonds, it is possible to greatly influence the polyamide's physical properties.[1] There are at least two routes to change the hydrogen bond density: either by changing the length of the aliphatic portions in the linear polyamide chains, which results in a change in the spatial separation between the amide groups, and hence an overall change in the hydrogen bond density,[2] or to replace the amide group with a different chemical unit that reduces the possibility of hydrogen bond formation but has similar structural features as the amide group. For the latter, a suitable comonomer would be piperazine, shown schematically in Figure 1. Since piperazine does not contain any amide hydrogens, it is unable to act as a hydrogen bond donor; thus, hydrogen bonding is reduced. However, piperazine can act as a hydrogen bond acceptor.[3,4]

Copolyamides of polyamide 2,14 (PA2,14) and piperazine (PApip,14)[3,4] were synthesized from 1,12-dodecanedicarboxylic acid and variable amounts of 1,2-ethylenediamine (1,2-EDA) and piperazine (pip). A range of copolyamides (PA2,14-*co*-pip,14) were prepared with varying piperazine content of 30−90 mol % as well as the homopolymers polyamide 2,14 (PA2,14) and polyamide pip,14 (PApip,14). The copolymers exhibited a decrease in melting and crystallization temperature with increasing piperazine content. Although the introduction of a rigid cyclic monomer usually leads to an increase in the melting temperature with respect to the homopolymer, the reduced ability of the piperazine units to form hydrogen bonds overrules this effect. It was also shown that up to a piperazine content of 62 mol % the PA2,14 and PApip,14 units co-crystallize into a common crystal lattice, which differs only slightly from the PA2,14 crystal lattice.[4] For a piperazine content of 90 mol % and higher, the crystal structure was distorted from that of PApip,14. For an intermediate piperazine content of 70 and 82 mol %, the studies indicated a coexistence of the PA2,14 and PApip,14 crystal structures. It was further concluded that the piperazine rings incorporated into the copolyamides were oriented parallel to the hydrogen-bonded sheets, the sheets being shifted parallel to one another.

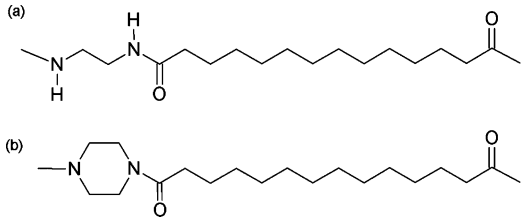

Figure 1. Chemical structure of (a) 1,2-ethylenediamine-based and (b) piperazine-based repeat units.

In the studies mentioned above,[3] the crystal structures of the homopolymers and the copolymers were only investigated at room temperature. It is known, however, that many polyamides show a Brill transition[5−7] upon heating. The Brill transition entails a solid-state crystalline transformation from a low-temperature triclinic to a high-temperature pseudohexagonal phase, as shown by the fact that the (100) reflection related to

[†] Laboratory of Polymer Technology, Eindhoven University of Technology.
[‡] Rutherford Appleton Laboratory.
[§] Free University of Brussels.
[⊥] Laboratory of Polymer Chemistry, Eindhoven University of Technology.
[||] Dutch Polymer Institute.

10.1021/ma0526903 CCC: $33.50
Published on Web 03/01/2006

the interchain/intrasheet distance and the (010)/(110) reflection related to the intersheet reflection merges into a single reflection. The true nature of the Brill transition is still a matter of debate. Initially, it was believed that the two-dimensional hydrogen-bonded sheets in the triclinic structure change to form a three-dimensional hydrogen-bonded network between the sheets.[8,9] Later it was proposed[10,11] that the high-temperature form is also triclinic with the hydrogen bonds in the sheets with the projection along the *c*-axis having a hexagonal symmetry. Many groups[12−15] have adopted the model that the hydrogen-bonded sheet structure is maintained throughout the Brill transition. Additionally, the Brill transition shows hysteresis upon heating and cooling,[16] suggesting a first-order process. An endothermic peak in DSC traces at the Brill transition has only been reported for polyamide crystals crystallized from solution.[16,17] This was attributed to the more uniform crystals obtained by solution crystallization as opposed to melt crystallization. Additionally, the Brill transition is strongly dependent on molecular structure and crystallization conditions.[16] Therefore, the Brill transition should be affected by the incorporation of a second diamide (i.e., piperazine) into the polyamide chain, both due to the possible influence on the crystal structure and, more importantly, due to the decrease in the hydrogen bond density. The present work therefore investigates the behavior upon heating of the homopolymers PA2,14 and PApip,14 and the copolymers PA2,-14-*co*-pip,14 using high-resolution WAXD, simultaneous SAXS/WAXD, and Fourier transform infrared (FTIR) spectroscopy. With these experiments we aim to understand the origin of the Brill transition in polyamides in general.

Experimental Section

a. Materials. The homopolymers PA2,14 and PApip,14 as well as the copolymers PA2,14-*co*-pip,14 were synthesized via a polycondensation reaction of 1,12-dodecanedicarbonyl dichloride and varying amounts of 1,2-ethylenediamine and piperazine as described elsewhere.[3] The piperazine-based copolyamides used in this study have a piperazine molar fraction of 0.30, 0.46, 0.54, 0.62, 0.82, and 0.90. These copolymers are referred to as coPA 0.30 through to coPA 0.90.

b. High-Resolution WAXD. High-resolution WAXD experiments were performed on the materials science beamline (ID11),[18] situated at the European Synchrotron Radiation Facility (ESRF), Grenoble, France (wavelength 0.5344 Å). The WAXD experiments were performed on ID11 because they give greater resolution than the WAXD measurements recorded using simultaneous SAXS/WAXD performed on the high brilliance beamline ID02. The powder samples, extracted after synthesis, were placed in 1 mm diameter Lindemann tubes and inserted within an aluminum holder attached to a Linkam TMS94 hot stage and controller; a hole in both the holder and the silver block of the heater allowed the X-ray beam to be transmitted though the sample. The samples were initially melted and then cooled to room temperature at a constant rate of 10 °C/min. Two-dimensional X-ray diffraction patterns using a 10 s exposure time were collected at 2 °C intervals (every 12 s) during the second heating of the samples at a rate of 10 °C/min. Silicon was used to calibrate the sample-to-detector distance. All diffraction patterns were corrected for spatial distortions and integrated to give intensity against 2θ.

c. Simultaneous SAXS/WAXD. Fresh samples of each of the copolymers and homopolymer were sealed in aluminum DSC pans and heated in a thermal analysis Q1000 DSC to temperatures well above (at least 15 °C) the respective melting temperatures of the polymers investigated and cooled to room temperature at 10 °C/min. This was performed twice for each sample. After this thermal pretreatment, the samples were scraped out of the DSC pans and placed in 2 mm diameter Lindemann capillaries. Time-resolved simultaneous SAXS/WAXD measurements (with X-ray energy of 12 keV ($\lambda = 0.9951$ Å) and 300 μm beam size) were performed at the high brilliance beamline (ID02),[19] at the ESRF, during heating at 10 °C/min from 50 °C to the melt and cooling from the melt to 50 °C on a Linkam TMS94 hot stage. The X-ray patterns were collected every 30 s with an exposure time of 1 s. A silicon standard was used to calibrate the WAXD sample-to-detector distance, and Lupolen was used for the SAXS sample-to-detector distance. All diffraction patterns were corrected for absolute intensity and integrated to give intensity against q. The SAXS results were Lorentz corrected; i.e., the intensity data were multiplied by q^2. The position, intensity, and FWHM of the crystalline peaks in the WAXD patterns were fitted using a Lorentzian function for each crystalline peak. Additionally, the fitting function contained a linear term to account for residual scattering arising from the background and the Lindemann tube. The melting end point and the crystallization onset temperatures observed during the DSC measurements were used to calibrate the Linkam hot stage.

d. FTIR. All samples were heated to the melt on a zinc selenium disk and cooled to room temperature at 10 °C/min using a Linkam TMS94 hot stage. Immediately after this pretreatment, FTIR spectra, all averages of 128 scans, were collected using a Bio-Rad FTS6000 spectrometer with a resolution of 2 cm^{-1}. Subsequently, each sample was heated in situ on a Linkam TMS94 hot stage at 10 °C/min in 10 °C steps from room temperature to just above their melting temperatures, and FTIR spectra were collected every 10 °C. During data collection, the temperature was kept constant. The resulting spectra were scaled to the area under the methylene bands between 3000 and 2800 cm^{-1}.

Results and Discussion

High-Resolution WAXD. Figure 2 shows a stacked plot of intensity against 2θ integrated from the WAXD patterns collected on the materials science beamline ID11 at the ESRF while heating the homopolymers PA2,14 and PApip,14 and the copolymer coPA 0.54 from 30 °C to the melt. For clarity, Figure 2a,b shows two different 2θ ranges (1−2.5° and 5−9°, respectively, for wavelength 0.5344 Å) for the homopolymer PA2,14. On heating, the diffraction peak at $2\theta = 1.6°$ shown in Figure 2a, corresponding to the (001) reflection, remains virtually constant up to the melt (242 °C), whereas the peak at $2\theta = 7.4°$, corresponding to the interchain (100) reflection, and the peak at $2\theta = 7.8°$, corresponding to the intersheet (010)/(110) reflection, merge into a single reflection (see Figure 2b). The merger shown in Figure 2b is a gradual transition spread over a temperature region of ∼35 °C.

Figure 2c,d shows a different behavior for coPA 0.54. The (001) reflection shown in Figure 2c remains constant up to melting (212 °C), and the interchain (100) and intersheet (010)/(110) reflections shown in Figure 2d merge to an extent that they cannot be deconvoluted. Compared to Figure 2b, the intersheet (010)/(110) reflection broadens on heating without its complete merger into the interchain (100) reflection. The presence of reminiscence prior to melting suggests some remainder of the room temperature phase at high temperatures with different interchain (100) and intersheet (010)/(110) distances and without its complete transformation into the pseudohexagonal phase. This difference in behavior between PA2,14 and coPA 0.54 may be attributed to the increased rigidity of the polymer chain by the introduction of piperazine rings. Finally, Figure 2e,f shows the diffraction patterns obtained for the homopolymer PApip,14. The (001) reflection shown in Figure 2e has moved to higher 2θ values in comparison to Figure 2a,c. This peak also remains constant in position up to melting (142 °C). Unlike the diffraction peaks shown in Figure 2b,d, the intersheet (010)/(110) ($2\theta = 8.2°$) and interchain (100) ($2\theta = 6.6°$) reflections shown in Figure 2f do not merge into a single reflection prior to melting but remain virtually constant in position right up to melting. The diffraction patterns in Figure

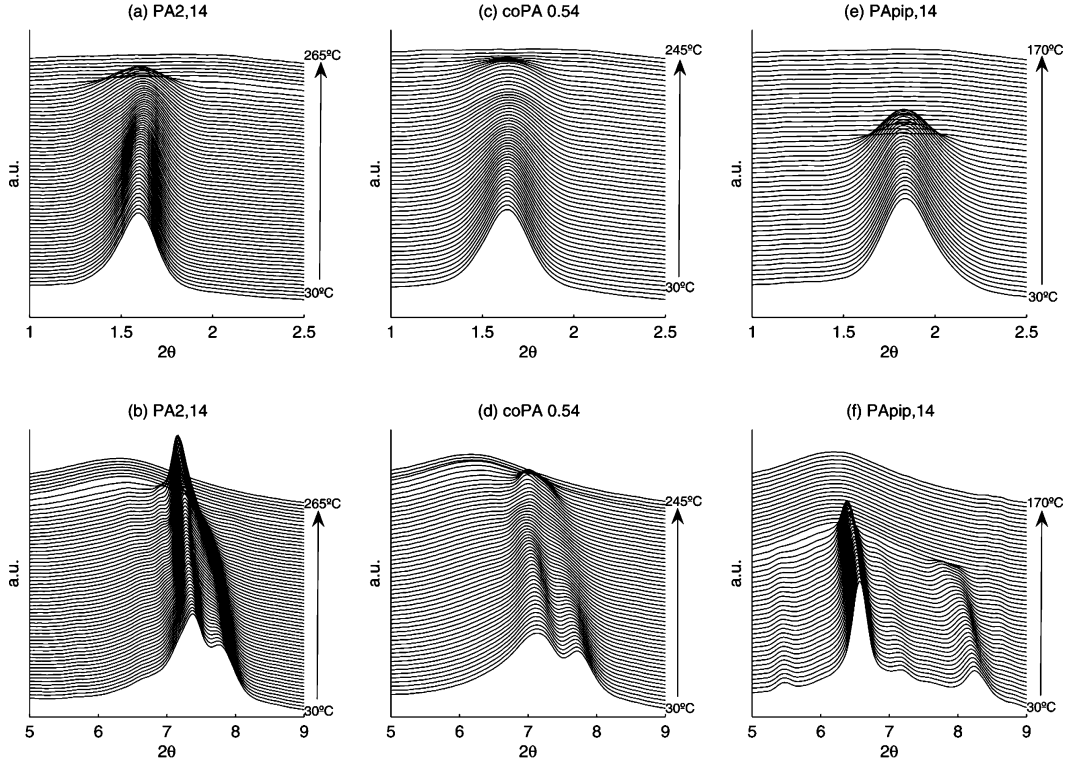

Figure 2. WAXD measurements obtained on heating PA2,14 (a, b), coPA 0.54 (c, d), and PApip,14 (e, f) from 30 °C to the melt at 10 °C/min. The diffraction peak observed in (a, c, and e) is the (001) reflection, whereas the two reflections in (b, d, and f) are the intersheet (010)/(110) ($2\theta = 7.8°$ in b) and interchain (100) ($2\theta = 7.4°$ in b) reflections, respectively. X-ray wavelength used is 0.5344 Å.

2f show two additional reflections at $2\theta = 7.2°$ and $2\theta = 5.5°$ that arise from the PApip,14 crystal structure, which is unknown at present. The observed changes in the diffraction patterns recorded at room temperature with increasing piperazine content are in accordance with our earlier publication.[4]

Simultaneous WAXD/SAXS. Figure 3 shows the data obtained from simultaneous WAXD and SAXS patterns collected on the high brilliance beamline ID02. The integrated WAXD patterns of intensity against q were fitted using a number of Lorentz functions and a linear background. The d-spacings were obtained from the fitted peak positions via the relation $d = 2\pi/q$. The WAXD pattern (Figure 3a) for the homopolymer PA2,14 at 50 °C corresponds well to data reported for this homopolymer at room temperature.[4,20] On heating, the interchain (100) ($d = 4.15$ nm) and intersheet (010)/(110) ($d = 3.92$ nm) reflections merge to an extent that no further deconvolution is feasible. The merger of the interchain (100) and intersheet (010)/(110) reflections shown in Figure 3a is similar to that seen in Figure 2b. This behavior is typically called the Brill transition in polyamides, and the temperature at which it occurs corresponds to the Brill temperature. On cooling from the melt the reverse behavior is seen, albeit at some undercooling. At ~25 °C below the melting point, the homopolymer crystallizes, resulting in a single reflection which splits into two reflections on further cooling. The WAXD patterns for coPA 0.30 (not shown) up to coPA 0.62 also show a Brill transition; however, coPA 0.82 and coPA 0.90 (not shown) are similar to that of the homopolymer PApip,14, where the intersheet (010)/(110) and interchain (100) reflections do not merge into a single reflection prior to melting. Figure 4 summarizes the Brill transition temperatures on heating and cooling for the various (co)polyamides investigated. As a reference, the temperatures of the end of melting endotherm (denoted melting temperature T_m) from DSC measurements and the detection of the onset of crystallization (T_c) from WAXD for the (co)polyamides[3] are also given. The Brill transition temperature remains approximately constant, on both heating and cooling, up to a piperazine content of 62 mol %. On heating the average Brill transition temperature is 165 °C and on cooling 147 °C. It is to be noted that the average Brill transition temperature on heating and cooling for these lower piperazine content copolymers is higher than T_m (or T_c) for coPA 0.82, coPA 0.90, and homopolymer PApip,14. This suggests that the reason that the Brill transition is not observed in coPA 0.82, coPA 0.90, and homopolymer PApip,14 is because the Brill transition temperature occurs at a temperature higher than T_m.

In Figure 3, the peak position of the SAXS patterns at 50 °C shows an increase with increasing piperazine content, which was also noted in the previous study.[4] On heating, all the (co)polyamides show an increase in lamellar thickness, often by twice its initial value, i.e., doubling in the SAXS peak position, just before melting as compared to the starting position at 50 °C. It is to be noted that while the lamellar thickness increases to twice the initial value, no considerable changes in crystallinity are observed, as evident from the corresponding WAXD patterns (see Figure 2). The homopolymer PA2,14 and copolyamides up to 62 mol % piperazine content show that above 165 °C (above the Brill transition temperature) the SAXS peak position changes more rapidly with increasing temperature (see Figure 3b,d). For the coPA 0.82, coPA 0.90 (not shown), and for the homopolymer PApip,14 the SAXS peak position changes more rapidly above ~110 °C. A remarkable observation is that polymers with high piperazine content do not show the Brill transition, although lamellar thickening occurs similarly to the copolymers that do show the Brill transition. The corresponding WAXD patterns for the high piperazine content (co)polymers do not suggest any changes in crystallinity or a phase transition around 110 °C (see Figure 2e,f).

After cooling from the melt the SAXS peak at 50 °C is positioned slightly higher than before heating. Because of

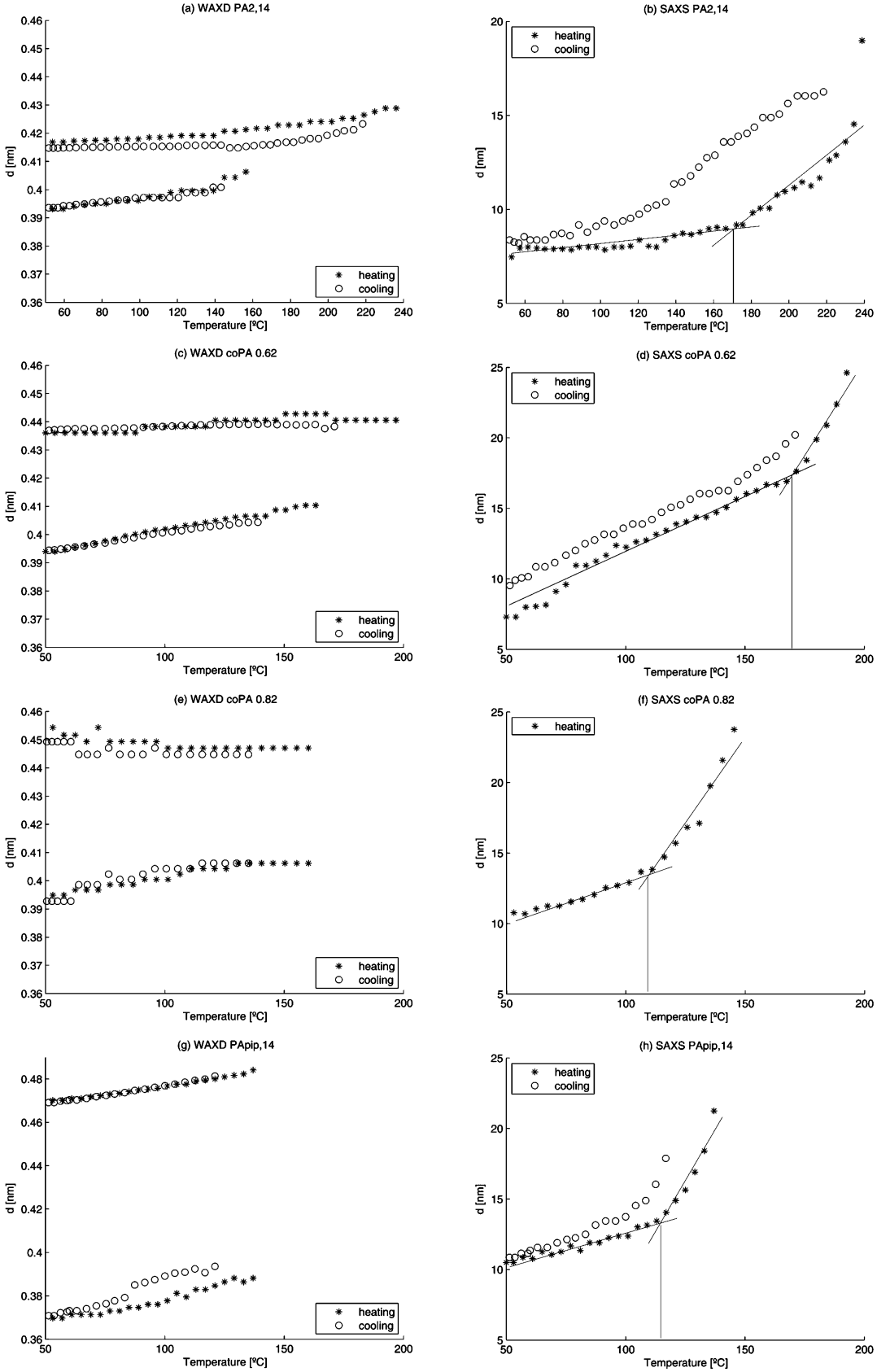

Figure 3. Simultaneous WAXD (a, c, e, g) and SAXS (b, d, f, h) of the homopolymers PA2,14 and PApip,14 and the copolymers coPA 0.62 and coPA 0.82 during heating from 50 °C to the melt and successive cooling from the melt to 50 °C at 10 °C/min. The Brill transition is observed up to a piperazine content of 62 mol %. The Brill transition temperature reported in Figure 4 has been determined from such data as reported here. The last data point for the (010)/(110) reflection in (a) and (c) for PA2,14 at 164 °C and coPA 0.62 at 159 °C, respectively, corresponds to the Brill transition temperature on heating. This is the last data point where deconvolution of the interchain (100) and the intersheet (010)/(110) reflections can be made. The lines over the SAXS heating runs serve as a guide to the eye. Because of detector problems, no SAXS pattern is available for the cooling run of coPA 0.82.

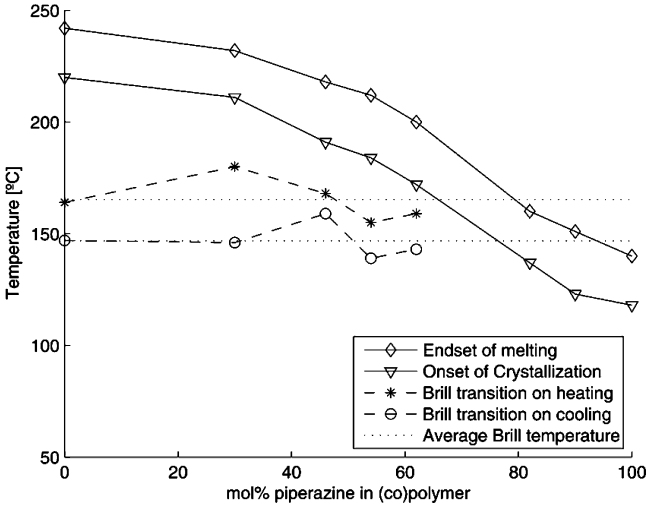

Figure 4. Brill transition temperature on heating and cooling over a range of molar piperazine fractions. The endset of melting and the onset of crystallization temperatures are also given. All lines serve as a guide to the eye.

problems with the detector, no SAXS patterns could be collected on cooling of coPA 0.82. On the basis of the WAXD patterns, Figure 2, it is expected that the SAXS cooling run of coPA 0.82 will follow a similar behavior as the SAXS cooling run of PApip,14. Our previous study[4] showed that the crystal structure in the recrystallized (co)polyamides still relaxes at room temperature and that this relaxation is only observed in the large repeat distance of the lamellar stacking and not in the interchain (100) and intersheet (010)/(110) distances. This relaxation process explains why the SAXS peak at 50 °C in the copolyamides is at a higher position directly after crystallization from the melt than before heating to the melt. Prior to melting the samples were allowed to relax at room temperature for nearly a week.

A sudden shift in the temperature required for lamellar thickening from 165 to 110 °C occurs with an increase in the piperazine content from 62 to 82 mol %, as shown in Figure 3. This sudden shift correlates well with the sudden changes in the interchain (100) and intersheet (010)/(110) distances observed with an increasing amount of piperazine content from 62 to 82 mol %, summarized in Figure 3 of ref 4 and in the *d* values observed at 50 °C shown in Figure 3a,c,e,g.

The authors are aware that determination of the true *d* values and the Brill transition requires investigation on single crystals. In a recent publication,[21] we have shown that polyamide 4,6 can be dissolved in water and single crystals can be obtained from the water solution. This dissolution phenomenon appears to hold generality in the aliphatic hydrogen-bonded polymers. Our ongoing research also suggests that copolyamide single crystals, similar to polyamide 4,6, can be obtained from a water solution. In a coming publication it will be possible for us to determine the unit cell parameters.

FTIR. Figure 5 shows the FTIR spectra collected for the polymers used in this study at 30 °C. All spectra were normalized relative to the area under the methylene bands between 3000 and 2800 cm^{-1} which will be invariant in this range of copolymers. Figure 5a shows the frequency range from 3500 to 2800 cm^{-1}. With increasing piperazine content, the bands at 3303, 3215, and 3085 cm^{-1} show a strong decrease, whereas a band at 3005 cm^{-1} appears at higher piperazine content. The bands at 3303, 3215, and 3085 cm^{-1} are associated with NH stretch vibrations, and those at 3215 and 3085 cm^{-1} are also associated with amide I and II overtones.[22] The

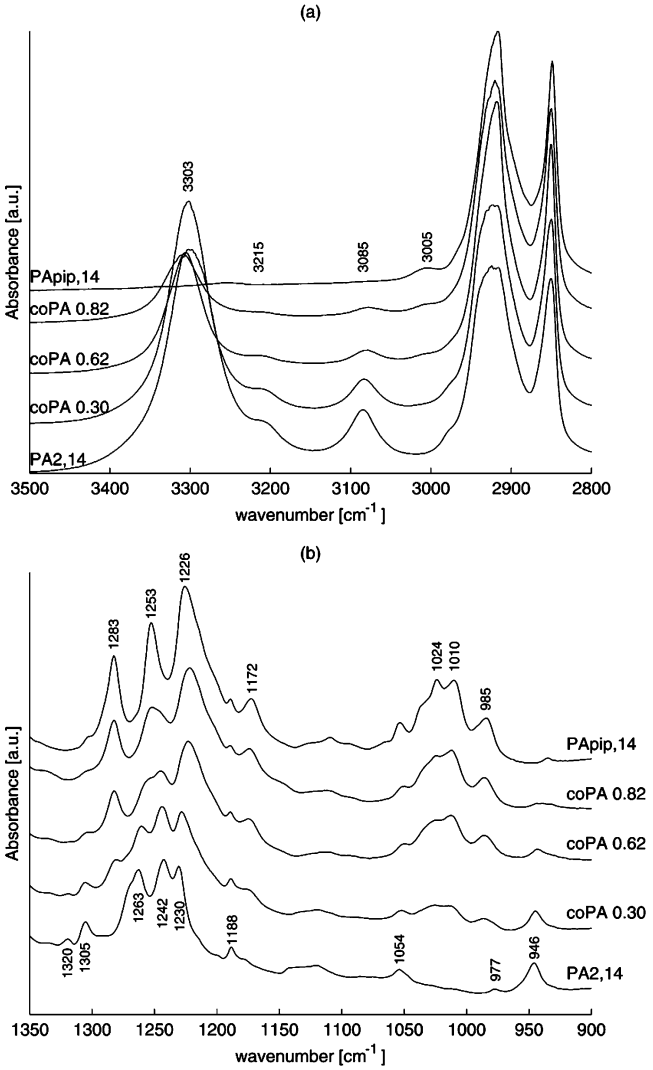

Figure 5. FTIR spectra of homopolymers PA2,14 and PApip,14 and copolyamides coPA 0.30, coPA 0.62, and coPA 0.82 recorded at 30 °C: (a) frequency range 3500−2800 cm^{-1} and (b) 1350−900 cm^{-1}.

reduction in the NH stretch bands is in line with the decreasing amount of NH groups with increasing piperazine content, whereas the band appearing at 3005 cm^{-1}, which becomes more apparent with increasing piperazine content, is most likely due to the methylene groups in the piperazine rings.

Figure 5b shows the FTIR spectra in the frequency range from 1350 to 900 cm^{-1}. Close inspection of the reflections present in this region leads to the observation that there are several bands that can be specifically assigned to the homopolymers PA2,14 and PApip,14, respectively. Additionally, there are bands that are common to both homopolymers. Specific bands that are associated with the homopolymer PA2,14 are 946, 977, 1230, 1242, 1263, and 1320 cm^{-1}. The bands associated with the homopolymer PApip,14 are 985, 1010, 1024, 1172, 1226, 1253, and 1283 cm^{-1}. Bands common to the both homopolymers are 1054, 1188, and 1305 cm^{-1}. As expected, depending on the piperazine content, the copolyamides show either the bands associated with the homopolymer PA2,14 (see coPA 0.30 in Figure 5b), the homopolymer PApip,14 (see coPA 0.82 in Figure 5b), or both (see coPA 0.62 in Figure 5b).

Figure 6 shows the FTIR spectra obtained in the frequency range 1350−900 cm^{-1} while heating the homopolymers PA2,14 and PApip,14 and the copolyamides coPA 0.30 and coPA 0.82 from 30 °C to the melt. Figure 6a shows the FTIR

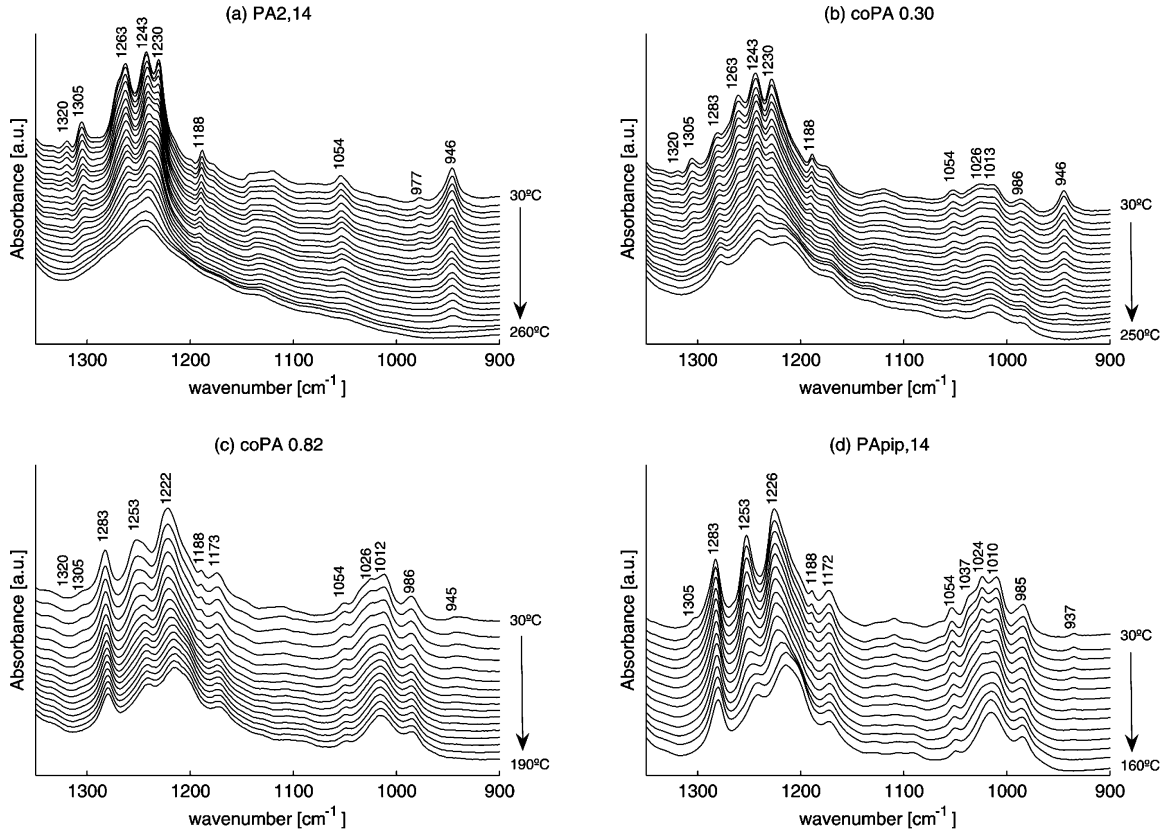

Figure 6. FTIR measurements of homopolymers PA2,14 and PApip,14 and copolyamides coPA 0.30 and coPA 0.82 on heating from 30 °C to the melt at 10 °C/min at regular intervals of 10 °C.

spectra for the homopolymer PA2,14 at different temperatures. On heating, the bands at 977, 1054, 1188, 1230, 1305, and 1320 cm^{-1} arising from the bending, wagging, and rocking vibrations of the methylene segments[23,24] disappear between 150 and 180 °C. This is the same temperature region where the Brill transition is anticipated; for comparison, see Figures 2b and 3a. For simplicity, these bands are therefore referred to as Brill bands; however, the lamellar thickening observed in the SAXS pattern for PA2,14 also occurs in this temperature region. Therefore, it is possible that some of the Brill bands seen here may be associated with the lamellar thickening and not with the Brill transition, but it is not possible to distinguish between the two effects from these FTIR spectra alone. On further heating, the bands at 946, 1243, and 1263 cm^{-1} broaden considerably or disappear altogether on melting and are therefore associated with the crystalline phase. The bands at 1243 and 1263 cm^{-1} are the amide III bands coupled with the out-of-plane methylene motions, whereas the band at 946 cm^{-1} is the amide IV vibration.[24−26]

Figure 6d shows the FTIR spectra for the homopolymer PApip,14 on heating from 30 °C to the melt. On heating from 30 °C, the bands at 1188 and 1305 cm^{-1} disappear between 100 and 110 °C, i.e., in the temperature region where the change in the lamellae thickness is observed in the SAXS patterns (see Figure 3h). On heating to the melt, the bands at 985, 1010, 1024, 1037, 1054, 1172, 1226, 1253, and 1283 cm^{-1} broaden.

The bands that disappear at the Brill transition in the homopolymer PA2,14 (Figure 6a) are also present in the homopolymer PApip,14 (Figure 6d), with some changes in PApip,14. The methylene band at 977 cm^{-1} in PA2,14 is now present at 985 cm^{-1} in PApip,14, the band at 1230 cm^{-1} at 1226 cm^{-1}, and the band at 1320 cm^{-1} is absent in PApip,14. These changes are due to the differences in chemical structure and an increased rigidity of the main chain in the homopolymer PApip,14 when compared to the homopolymer PA2,14.

In previous studies,[26,27] performed on several polyamides (PA10,10; PA6,12; PA6,10), it was found that during the Brill transition conformational disorder occurs in the methylene sequences. With increasing temperature the intermolecular hydrogen bonding between the amide groups weaken, although it is retained up to melting. The methylene sequences between the NH groups are found to become more disordered than the methylene sequences between the CO groups. To model the changes in the FTIR spectra close to the Brill transition, the methylene units adjacent to the amide groups needed to be decoupled from the remaining methylene segments. It was concluded that even after the Brill transition hydrogen bonding is retained, thus making the chain rotation along the *c*-axis in the pseudohexagonal phase impossible. Structural changes in the methylene parts of the molecular chains were observed. Similar observations are reported by others.[12,15]

For the homopolymer PA2,14 shown in Figure 6a the vibrational bands associated with the methylene groups next to the CO groups are 977 and 1054 cm^{-1} and the bands associated with the methylene groups next to the NH groups are 1230 and 1320 cm^{-1}.[25,26] On heating, all these bands decrease in intensity and ultimately disappear above the Brill transition but below the melting point. However, the methylene bands next to the NH group decrease faster than the bands next to the CO groups. These observations are in agreement with the results reported by Tashiro et al.[26,27]

Unlike in PA2,14, in PApip,14, the vibrational bands of the methylene groups next to the N (1226 cm^{-1}) and the CO (985 and 1054 cm^{-1}) remain even after melting. These observations suggest that in PApip,14 the rigidity along the main chain inhibits the complete disappearance of these bands, although

broadening and slight shifting to higher frequencies of these bands close to the melting point are noticed.

However, similar to PA2,14, in PApip14 the bands at 1188 and 1305 cm^{-1} disappear but at lower temperatures, i.e., between 100 and 110 °C (see Figure 6d). These bands are related to the main-chain methylene stretching and wagging motions.[25] Considering the absence of the Brill transition in PApip,14 these bands are not immediately related to the Brill transition. The disappearance of these two bands coincides with the change in the lamellar thickness observed in the SAXS patterns for all the polymers investigated. Conformational changes in the main chain combined with the lamellar thickening suggest the presence of enhanced chain mobility along the *c*-axis. Increased chain mobility would lead to the disappearance of the trans conformers, i.e., the methylene main chain bands at 1188 and 1305 cm^{-1}. Similar chain mobility above the Brill transition has been observed in nylons[28] as well as in linear polyethylenes[29] above room temperature, where regular sedimentation of crystals occurs.

Figure 6b shows the FTIR spectra for the coPA 0.30 and Figure 6c for the coPA 0.82 on heating from 30 °C to melt. The FTIR spectra for coPA 0.30 follow the same behavior as that of the homopolymer PA2,14, and the spectra of coPA 0.82 follow the same behavior as the homopolymer PApip,14.

Conclusions

The thermal behavior of homopolymers PA2,14 and PApip,-14 and their copolyamides, varying from 30 up to 82 mol % piperazine, are investigated using DSC, WAXD, SAXS/WAXD, and FTIR. These studies provide an insight into the effect of incorporating a secondary diamide that reduces the number of hydrogen bonds within the crystal lattice, thus is likely to influence the Brill transition temperature. The observations are that the Brill transition temperature remains independent of the piperazine content up to 62 mol % piperazine in the copolymer. Up to a piperazine content of 62 mol % an average Brill transition temperature of 165 °C is observed on heating and 147 °C is observed on cooling. FTIR measurements show the disappearance of the 1188 and 1305 cm^{-1} vibrational bands, suggesting disorder in the trans planar zigzag conformations of the methylene segments of the main chain. In PA2,14 this conformational disorder occurs between 150 and 180 °C, whereas in PApip,14 the disorder occurs between 100 and 110 °C. The higher temperature required for the disorder in PA2,14 compared to PApip,14 is a consequence of the presence of hydrogen bonding in PA2,14. With the disappearance of the conformational bands enhanced chain mobility along the *c*-axis is seen which leads to lamellar thickening, observed in SAXS, where ultimately the lamellae thicken to twice their initial, room temperature value. The striking observation is that this increase in lamellar thickening is independent of piperazine content up to 62 mol %. A closer look at the methylene bands 1188 and 1305 cm^{-1} suggests that with increasing piperazine content, i.e., as the number of hydrogen bonds decrease, changes in the intensity of these methylene bands occur at lower temperatures followed by their complete disappearance in the region of 150−180 °C.

When the Brill transition occurs in PA2,14, the methylene bands next to the CO group (977 and 1054 cm^{-1}) and NH group (1230 and 1320 cm^{-1}) disappear. Similar changes are registered in the copolymers up to piperazine content of 62 mol %. From 82 mol % onward these bands do not disappear even in the melt of the copolymer or the homopolymer PApip14.

Combining the FTIR and X-ray diffraction data, it can be stated that with the disappearance of the trans conformers of the methylene chain segments in PA2,14 and the piperazine copolymers chain mobility along the *c*-axis arises once the methylene unit next to the carbonyl group is able to twist although hydrogen bonding is likely to be retained. These observations are in agreement with previous studies.[12,15,26,27] In PApip14 where the hydrogen bonding is absent the chain mobility occurs earlier, and twisting is not observed due to the piperazine rings that are oriented parallel to the hydrogen-bonded sheets.[4]

Acknowledgment. The authors thank the ESRF for beamtime on the high brilliance beamline ID02, as part of the long-term proposal number SC1279, and for beamtime on the materials science beamline ID11, as part of proposal no. ME161. The authors also thank Silvia Capelli and Peter Boesecke for their expertise and support during the X-ray measurements. The authors thank Jan Devroede for synthesizing the piperazine-based copolymers used in this study.

References and Notes

(1) Ehrenstein, M.; Dellsperger, S.; Kocher, C.; Stutzmann, N.; Weder, C.; Smith, P. *Polymer* **2000**, *41*, 3531.
(2) Brydson, J. *Plastic Materials*, 7th ed.; Butterworth-Heinemann: Oxford, UK, 1999.
(3) Vanhaecht, B.; Devroede, J.; Willem, R.; Biesemans, M.; Goonewardena, W.; Rastogi, S.; Hoffmann, S.; Klein, P. G.; Koning, C. E. *J. Polym. Sci., Part A: Polym. Chem.* **2003**, *41*, 2082.
(4) Hoffmann, S.; Vanhaecht, B.; Devroede, J.; Bras, W.; Koning, C. E.; Rastogi, S. *Macromolecules* **2005**, *38*, 1797.
(5) Brill, R. *J. Prakt. Chem.* **1942**, *161*, 49.
(6) Jones, N. A.; Atkins, E. D. T.; Hill, M. J.; Cooper, S. J.; Franco, L. *Macromolecules* **1997**, *30*, 3569.
(7) Jones, N. A.; Atkins, E. D. T.; Hill, M. J.; Cooper, S. J.; Franco, L. *Polymer* **1997**, *38*, 2689.
(8) Brill, R. *Makromol. Chem.* **1956**, *18/19*, 294.
(9) Schmidt, G. F.; Stuart, H. A. *Z. Naturforsch., A* **1958**, *13*, 222.
(10) Cannon, C. G.; Chappel, F. P.; Tidmarsh, J. I. *J. Text. Inst.* **1963**, *54*, T210.
(11) Colclough, M. L.; Baker, R. *J. Mater. Sci.* **1978**, *13*, 2531.
(12) Hirschinger, J.; Miura, H.; Gardner, K. H.; English, A. D. *Macromolecules* **1990**, *23*, 2153.
(13) Murthy, N. S.; Curran, S. A.; Aharoni, S. M.; Minor, H. *Macromolecules* **1991**, *24*, 3215.
(14) Itoh, T.; Yamagata, T.; Hasegawa, Y.; Hashimoto, M.; Konishi, T. *Jpn. J. Appl. Phys.* **1996**, *35*, 4474.
(15) Cooper, S. J.; Coogan, M.; Everall, N.; Priestnall, I. *Polymer* **2001**, *42*, 10119.
(16) Ramesh, C.; Keller, A.; Eltink, S. J. E. A. *Polymer* **1994**, *35*, 2483.
(17) Starkweather, H. W.; Jones, G. A. *J. Polym. Sci., Polym. Phys.* **1981**, *19*, 467.
(18) Kvick, A. *Nucl. Instrum. Methods Phys. Res. B* **2003**, *199*, 531.
(19) Urban, V.; Panine, P.; Ponchut, C.; Narayanan, T. *J. Appl. Crystallogr.* **2003**, *36*, 809.
(20) Li, Y.; Zhang, G.; Yan, D.; Zhou, E. *J. Polym. Sci., Part B: Polym. Phys.* **2002**, *40*, 1913.
(21) Rastogi, S.; Terry, A. E.; Vinken, E. *Macromolecules* **2004**, *37*, 8825.
(22) Jakes, J.; Krimm, S. *Spectrochim. Acta* **1971**, *27A*, 19.
(23) Vasanthan, N.; Murthy, N. S.; Bray, R. G. *Macromolecules* **1998**, *31*, 8433.
(24) Cui, X.; Li, W.; Yan, D. *Polym. Int.* **2004**, *53*, 2031.
(25) Cui, X.; Yan, D. *J. Polym. Sci., Part B: Polym. Phys.* **2004**, *42*, 4017.
(26) Yoshioka, Y.; Tashiro, K.; Ramesh, C. *Polymer* **2003**, *44*, 6407.
(27) Tashiro, K.; Yoshioka, Y. *Polymer* **2004**, *45*, 6349.
(28) Dreyfuss, P.; Keller, A. *J. Macromol. Sci.* **1970**, *B4*, 811.
(29) Rastogi, S.; Spoelstra, A. B.; Goossens, J. G. P.; Lemstra, P. J. *Macromolecules* **1997**, *30*, 7880.

MA0526903